Image Anal Stereol 2024;43: 203-210 doi: 105566/ias.3332
Original Research Paper

ANALYSIS-ASSOCIATED FACTORS INTERFERING WITH DIFFUSION TENSORS OF PERIPHERAL NERVES

LUKA PUŠNIK✉,[1], LUCIJA LAUBRY[1], IGOR SERŠA[1 2], ARMIN ALIBEGOVIĆ[3], ERIKA CVETKO[1], ŽIGA SNOJ[4,5], NEJC UMEK[1]

[1]Institute of Anatomy, Faculty of Medicine, University of Ljubljana, Korytkova 2, 1000 Ljubljana, [2]Department of Condensed Matter Physics, Jožef Stefan Institute, Ljubljana, Slovenia, [3]Institute of Forensic Medicine, Faculty of Medicine, University of Ljubljana, Korytkova 2, 1000 Ljubljana, Slovenia; Slovenia, [4]Department of Radiology, Faculty of Medicine, University of Ljubljana, Ljubljana, Slovenia, [5]Institute of Radiology, University Medical Centre Ljubljana, Ljubljana, Slovenia.

e-mail: luka.pusnik@mf.uni-lj.si, lucija174@gmail.com, igor.sersa@ijs.si, armin.alibegovic@mf.uni-lj.si, erika.cvetko@mf.uni-lj.si, ziga.snoj@gmail.com, nejc.umek@mf.uni-lj.si

(Received July 17, 2024; revised September 9, 2024; accepted October 9, 2024)

ABSTRACT

Diffusion tensor imaging (DTI) enables a non-invasive assessment of tissue architecture based on water diffusion. High-resolution magnetic resonance imaging (MRI) systems have enhanced the visualization of nerve compartments. This study investigates the influence of region of interest (ROI) selection on DTI indices in ex vivo peripheral nerves. Cadaveric median nerves (n=10) were harvested and immersed in fluorinated-carbon liquid, and 9-mm segments were scanned with a 9.4-T MRI system. Diffusion-weighted signals were summed, and diffusion tensors were calculated for anatomical compartments using different delineation techniques. Following the initial scan, five samples were scanned for a second time using an identical protocol. The analysis showed that the inclusion of an inert background into the ROI significantly reduces fractional anisotropy (FA). Significant differences in diffusion tensors were observed between the initial and intermediate segments, with FA and mean diffusivity (*MD*) differing by as much as 25.2% and 25.6%, respectively. Tracing the fascicles without the interfascicular epineurium exhibited an 8.8% lower FA compared to the delineations of the epineurium. Second MRI scans showed significant changes in diffusion tensors with higher eigenvalues D_1-D_3 and *MD*; along with lower FA. In conclusion, the intermediate portions of the nerve demonstrated greater consistency in DTI indices and are recommended for analysis over the initial portions. Using an inert liquid can minimize background effects, but the inherent diffusion properties of the tissue must be carefully considered. Prolonged scanning times can alter diffusion tensors, likely due to autolytic processes, underscoring the importance of consistent pre-scanning conditions and acquisition protocols. Additionally, maintaining consistency in delineations is paramount, regardless of whether the tracing method includes or excludes the interfascicular epineurium.

Keywords: diffusion tensor imaging; diffusion weighted imaging; fractional anisotropy; image analysis; nerve anatomy; peripheral nerve.

INTRODUCTION

Diffusion tensor imaging (DTI) is a quantitative imaging modality that enables non-invasive assessment of tissue architecture based on the anisotropic diffusion of water molecules within tissues. Although the technique was initially employed for central nervous system imaging, recent advances in hardware and software development have expanded its applications to other biological systems, including the peripheral nerves (Jeon *et al.*, 2018). Numerous DTI protocols have been established, facilitating the assessment of peripheral nerve injuries in rodent models and enabling the differentiation between intact, transected, and regenerating nerves (Lehmann *et al.*, 2010). Studies have demonstrated the high diagnostic accuracy of DTI in detecting peripheral nerve injuries in humans (Breckwoldt *et al.*, 2015; Gallagher *et al.*, 2015) and its potential for identifying peripheral neuropathies. Consequently, DTI of peripheral nerves may hold promise for diagnosing nerve entrapment syndromes or diabetic neuropathy (Chen *et al.*, 2023; Goyal *et al.*, 2022; Wang *et al.*, 2022).

Clinical MRI systems present challenges in imaging peripheral nerves due to their small caliber, resulting in limited image resolution. High-field MRI, which utilizes stronger magnetic fields than the standard 1.5-T or 3-T

systems, allows more precise delineation of finer structures such as nerve fascicles (Jeon *et al.*, 2018). Recently, high-field 7-T MRI systems have demonstrated the ability to depict interneural architecture with significantly improved signal-to-noise ratio. However, these systems are primarily utilized for research purposes due to their complexity, high cost, and the limited availability of reference data (Cosottini & Roccatagliata, 2021; Sveinsson *et al.*, 2022). To evaluate diffusion within the much smaller anatomical compartments of peripheral nerves, even stronger magnetic fields or special coils can be utilized. However, such protocols are typically limited to *ex vivo* conditions due to the need for high-sensitivity MRI probes, extended scanning times, and increased susceptibility to motion artefacts (Awais *et al.*, 2022).

The superior resolution of high-field MRI images enables a more detailed selection of regions of interest (ROI), particularly when considering perineural tissue or intraneural anatomical compartments. Nonetheless, the influence of ROI selection on diffusion tensor indices obtained with high-field MRI is not well understood. Preclinical 9.4-T high-field MRI systems have demonstrated large variability in diffusion tensors across different anatomical compartments of the peripheral nerves. These studies have shown that the interfascicular epineurium exhibits most isotropic diffusion, whereas the perineurium and fascicles have more anisotropic water movement (Awais *et al.*, 2022; Pušnik *et al.*, 2023). This study sought to further elucidate factors related to the ROI selection that could potentially interfere with diffusion tensor indices of peripheral nerves.

MATERIALS AND METHODS

Specimens and ethical approval

The nerve samples were obtained from ten cadavers during standard autopsy procedures at the Institute of Forensic Medicine, Faculty of Medicine, University of Ljubljana. Additionally, five samples previously utilized in a study employing a similar MRI protocol (Pušnik *et al.*, 2023) were included for histological cross-referencing. Limited data was available regarding the medical status of the cadavers. This study was approved by the National Medical Ethics Committee of the Republic of Slovenia (Permits No.: 0120–239/2020/3, 0120-536/2019/7).

Approximately 20-mm-long segments of median nerves were harvested from the mid-arm within 24 hours post-mortem. Each sample was shortened to a 9-mm-long segment, and the surrounding connective tissue was partly removed. Those segments were snap-frozen in liquid nitrogen and stored at -80 °C until acquisition.

Diffusion tensor imaging

The samples were placed in a glass tube filled with perfluorinated liquid (Galden SV110, Solvay, Brussels, Belgium). This liquid prevented desiccation during scanning and did not produce any MR signal (Snoj *et al.*, 2020). Magnetic resonance imaging has been conducted on 9.4-T wide-bore vertical superconducting magnet Jastec (Jastec Superconductor Technology, Tokyo, Japan) with 400 MHz proton NMR frequency connected to an NMR/MRI spectrometer (Tecmag, Houston TX, United States).

DTI imaging was performed with a three-dimensional (3D) pulsed gradient spin-echo (PGSE) imaging sequence in 19 different gradient directions with $b = 1150$ s/mm^2 and one T_2-weighted image without diffusion weighting ($b = 0$ s/mm^2). The scanning was performed with the following parameters: TE = 36 ms, TR = 880 ms δ =27 ms, Δ = 3 ms; G_0 = 260.7 mT/m, field of view (FOV) = 19 × 9.5 × 10 mm^3; slice thickness = 625 μm; no interslice gap; acquisition and reconstruction matrix = 256 × 128 × 16; and 4 signal averages. The temperature within the MRI was set at 20 ± 2 °C. Each sample was scanned independently, with a total scanning time of 40 hours per nerve sample.

Diffusion tensor calculations

Detailed image analysis was performed using using ImageJ software (National Institutes of Health, Bethesda, MD, USA). The analysis was conducted manually or with semi-automatic threshold detection, depending on the specific parameter being evaluated. ROIs were delineated using the ROI manager plugin and the measure function. The diffusion tensors of the delineated peripheral nerve components were then calculated as previously described (Awais *et al.*, 2022). In brief, the fascicles were recognized as hypointense oval to round tissue, surrounded by a thin layer of more hyperintense perineurium. The surrounding connective tissue was considered an interfascicular epineurium, while the outer rim represented the epineurium. To improve the signal-to-noise ratio of the diffusion-weighted imaging signals (in 19 different gradient directions), the diffusion-weighted signals of all voxels within the selected region were first summed, and then the diffusion tensor was calculated from these signals and diagonalized to obtain the corresponding diffusion eigenvalues (D_1, D_2, D_3) and eigenvectors (e_1, e_2, e_3) of the region. This approach yielded more accurate results for eigenvalues and eigenvectors than their direct calculation for each voxel, followed by their averaging over the selected region. From the known diffusion eigenvalues of the region, it was possible to further calculate two indices, namely the

mean diffusivity (*MD*) and the fractional anisotropy (*FA*) (Eq. 1 and Eq. 2). All the calculations were performed using a C programming language program, developed and previously described by the authors (Pušnik *et al.*, 2023).

$$MD = \frac{D_1 + D_2 + D_3}{3} \quad (1)$$

$$FA = \sqrt{\frac{3}{2}} \frac{\sqrt{(D_1 - MD)^2 + (D_2 - MD)^2 + (D_3 - MD)^2}}{\sqrt{D_1^2 + D_2^2 + D_3^2}} \quad (2)$$

Analysis of diffusion tensors

Five intermediate sections were randomly chosen from each nerve, and the nerve cross-sectional area was delineated in different fashions. Measurements were conducted by tracing the nerve cross-sectional areas (CSA) and then repeating the delineations with incrementally increased background proportions using the ROI manager and measure function. Each section was analyzed four times, based on the background proportion: without background (tracing only the nerve CSA), and with 25%, 50%, and 100% additional background. For the inter-slice variability analysis, the initial two and final two sections containing nerve had the nerve's CSA delineated. Their mean diffusion tensors were compared to the mean diffusion tensors calculated from five intermediate slices.

The impact of interfascicular epineurium on diffusion tensor indices was evaluated by comparing two tracing methods, each applied on five consecutive MRI sections of each nerve. These sections were the same as used for the background assessment. The initial tracing of fascicles included all fascicles combined, including the interfascicular epineurium, but without the surrounding connective tissue extending beyond the epineurium. The consequent delineations were performed by tracing the fascicles without the interfascicular epineurium. Additionally, each section had diffusion tensors calculated by delineating approximately ½ and ⅔ of randomly chosen nerve fascicles.

Second acquisition of samples

Straight after the initial scan, a second acquisition of five nerves was performed. The second MRI acquisition was made with an identical imaging protocol. The images of initial and second scan were cross-referenced and five cross-sections of each nerve were compared in the same fashion as described for the initial scan.

Fascicular ratio analysis: manual vs. threshold

Fascicular ratio (FR) was calculated as a quotient between net fascicular CSA and nerve CSA (Snoj *et al.*, 2024). Manual assessment of FR was performed by manually delineating the nerve and fascicles. The semi-automatic assessment was conducted using the threshold function, by incrementally adjusting the fascicle area and then calculating the FR.

Reference image effect on fascicle count

Histological analysis was conducted on five median nerve samples previously used in another experiment where diffusion tensor indices were calculated (Pušnik *et al.*, 2023). The samples were scanned using a similar MRI protocol. Immediately following MRI acquisition, the nerves were frozen in liquid nitrogen and sectioned into 10-µm-thick histological sections using a cryostat (Leica, CM 1950, Leica Microsystems GmbH, Wetzlar, Germany) for the purposes of this study. The sections were stained with hematoxylin and eosin, visualized using a Nikon Eclipse 80i microscope (Nikon, Tokyo, Japan), and captured under 40× magnification with the Microscope camera ODC 841 (Kern & Sohn, Balingen, Germany) at a resolution of 5440 × 3648 pixels. Five histological sections with minimal procedural artifacts and the greatest similarity in shape pattern to the corresponding T_2-weighted MRI images were selected for cross-referencing. A comparison of fascicle counts was performed through repeated evaluations of these sections, first without reference to the histological cross-sections and then with the histological cross-sections available for comparison.

Intra- and inter-rater agreement

Intra-rater and inter-rater agreement were assessed using intraclass correlation coefficients (ICC). One month after the initial evaluation, the nerve and fascicular areas of one section per nerve sample were re-delineated by the original evaluator. To calculate inter-rater agreement, the same sections were delineated by a second, independent evaluator. *FA*s were calculated from the delineated areas and compared using ICC as described below.

Statistical analysis

Data are presented as means with standard deviations or proportions, as appropriate. Statistical analysis and graphing were performed using GraphPad Prism 10 (GraphPad Software Inc., San Diego, CA, USA), while inter-rater and intra-rater agreement were calculated using SPSS (IBM Corp., Armonk, NY, USA). Intra-rater

and inter-rater reliability were analyzed using the two-way mixed ICC (absolute agreement, single measurement) and interpreted according to established guidelines (Koo & Li, 2016). Diffusion tensors were analyzed using repeated measures t-tests or repeated measures analysis of variance (ANOVA), depending on the number of groups being compared. To assess the variability of diffusion tensors between sections of the same nerve, the coefficients of variation of *FA* for shorter nerve portions were calculated and then compared using a repeated measures t-test (initial portion vs. intermediate portion). Differences were considered significant at *p*-values below 0.05.

RESULTS

To evaluate the influence of background effect on diffusion tensors, the nerves were analysed with varying proportions of the surrounding background. Nerves delineated with an additional 25% of surrounding background in the ROI exhibited a 2% lower *FA* compared to delineations without background ($p < 0.0001$), while those with a 100% surplus of background in the ROI showed a 7% decrease in *FA* (Table 1). Repeated measures ANOVA revealed significant differences between the measurements performed with varying proportions of surrounding background for all analyzed eigenvalues $D_{1\text{-}3}$, *MD*, and *FA* (all $p < 0.001$).

To test whether different portions of the samples differ in diffusion tensors, the initial and intermediate portions were compared. The interslice comparison showed significant differences between the initial and intermediate portions in all analysed diffusion tensors (all $p < 0.0001$), with intermediate portions exhibiting much higher *FA* values than initial. The differences in *FA* and *MD* differed up to 25.2% and 25.6%, respectively (Table 2). There were no correlations between changes in *FA* and *MD*. A repeated measure t-test showed that initial portions had significantly larger coefficients of variation over the intermediate portions ($p = 0.005$).

The influence of the interfascicular epineurium on the diffusion tensors of the nerve was evaluated using different delineation techniques. Fascicles had 8.8% higher *FA* compared to fascicles with interfascicular epineurium ($p < 0.0001$) (Table 3). Half fascicles or two-thirds of fascicles demonstrated similar values with non-significant differences compared to all fascicles. There was a strong positive correlation between the fascicular *FA* and *FA* of fascicles with interfascicular epineurium ($r = 0.98$; $p < 0.0001$).

To assess test-retest reliability of MRM acquisition, five samples were scanned again, and their diffusion tensors were compared. The analysis of the identical sections with second sample acquisition showed significant differences in eigenvalues $D_{1\text{-}3}$, *MD*, and *FA* (Table 4).

FR was calculated manually and using semi-automatic technique. Manual FR was 0.46 ± 0.09, while the semi-automatic FR was significantly higher, 0.53 ± 0.08 ($p = 0.0002$). The delineation of fascicles with referential histological images enabled the delineation of more fascicles (8.48 ± 4.73) compared to the blind assessment (8.00 ± 4.52) ($p < 0.001$; Fig. 1).

The intra-rater and inter-rater repeatability for diffusion tensor calculations from manually delineated nerve CSA and fascicular CSA was excellent in both assessed parameters (Table 5). The lowest agreement has been detected for the nerve fascicles compared between both raters.

Table 1. *Background effect on diffusion tensors*.

	D_1	D_2	D_3	*MD*	*FA*
CSA nerve	0.53 ± 0.22	0.35 ± 0.13	0.34 ± 0.12	0.41 ± 0.15	0.26 ± 0.05
CSA nerve with 25% background	0.51 ± 0.20	0.35 ± 0.13	0.33 ± 0.12	0.40 ± 0.15	0.25 ± 0.05
CSA nerve with 50% background	0.49 ± 0.19	0.34 ± 0.12	0.32 ± 0.12	0.38 ± 0.14	0.24 ± 0.05
CSA nerve with 100% background	0.48 ± 0.19	0.33 ± 0.12	0.31 ± 0.11	0.37 ± 0.14	0.24 ± 0.05

Data are presented as mean ± standard deviation, calculated from 10 median nerve samples, each with 4 different delineation techniques. CSA – cross-sectional area; D_x – eigenvalues [$\times 10^{-9}$ m^2/s]; *FA* – fractional anisotropy; *MD* – mean diffusivity [$\times 10^{-9}$ m^2/s].

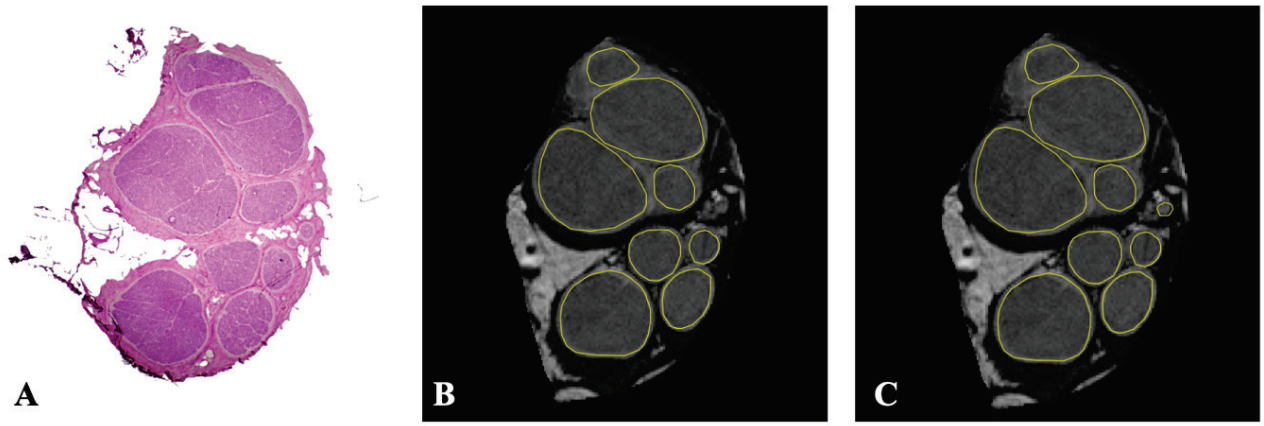

Figure 1. *Fascicle tracing process with the presence and absence of a referential histological image. Panel **A** depicts the histological section of the median nerve (haematoxylin and eosin, ×20 magnification, slice thickness = 10 μm), and panels **B** and **C**, the corresponding magnetic resonance microscopy section (slice thickness = 650 μm). Panel **B** displays the initial fascicle tracing with the evaluator blinded to the referential cross-section, while panel **C** demonstrates the re-delineation of fascicles with the evaluator unblinded to the referential histological section. Note the additional fascicle being recognized, consequently raising the total fascicle count. The CSA of additional fascicle is negligible compared to the sum of areas of the remaining fascicles.*

Table 2. *Inter-slice comparison of absolute differences in diffusion tensors between initial and intermediate portions.*

	ΔD_1 (%)	ΔD_2 (%)	ΔD_3 (%)	ΔMD (%)	ΔFA (%)
Nerve 1	0.11 (34.7)	0.09 (36.3)	0.09 (37.1)	0.10 (35.9)	0.01 (7.1)
Nerve 2	0.18 (19.6)	0.11 (17.5)	0.08 (15.3)	0.12 (18.0)	0.02 (7.7)
Nerve 3	0.10 (21.0)	0.07 (18.7)	0.08 (22.0)	0.08 (20.6)	0 (0)
Nerve 4	0.08 (11.8)	0.06 (12.1)	0.04 (8.9)	0.06 (11.1)	0.01 (3.0)
Nerve 5	0.02 (5.7)	0.02 (6.0)	0.02 (5.5)	0.02 (5.7)	0 (0)
Nerve 6	0.04 (7.2)	0.02 (4.6)	0.02 (7.1)	0.03 (6.5)	0.01 (2.3)
Nerve 7	0.06 (7.6)	0.02 (2.7)	0.01 (2.9)	0.03 (5.0)	0.03 (9.1)
Nerve 8	0.16 (19.1)	0.07 (13.2)	0.06 (11.8)	0.08 (12.6)	0.08 (25.2)
Nerve 9	0.18 (26.8)	0.11 (24.5)	0.11 (24.8)	0.13 (25.6)	0.02 (6.2)
Nerve 10	0 (0)	0 (1.1)	0.01 (6.0)	0 (1.5)	0.02 (5.4)
Mean [range]	0.09 [0-0.18]	0.06 [0-0.11]	0.05 [0-0.11]	0.06 [0-0.13]	0.02 [0-0.08]

Data are presented as (absolute) mean differences between four initial and five intermediate sections with proportions. Data are presented for each nerve separately. D_x – eigenvalues [$\times 10^{-9}$ m^2/s]; FA – fractional anisotropy; MD – mean diffusivity [$\times 10^{-9}$ m^2/s].

Table 3. *Analysis of fascicular diffusion tensors with different delineation techniques.*

	D_1	D_2	D_3	MD	FA
All fascicles	0.97 ± 0.13	0.58 ± 0.10	0.53 ± 0.10	0.69 ± 0.11	0.34 ± 0.05
½ of fascicles	0.93 ± 0.11	0.57 ± 0.11	0.52 ± 0.10	0.69 ± 0.11	0.34 ± 0.05
⅔ of fascicles	0.95 ± 0.16	0.57 ± 0.10	0.52 ± 0.10	0.68 ± 0.12	0.33 ± 0.04
Fascicles with IE	0.86 ± 0.14	0.53 ± 0.10	0.49 ± 0.10	0.63 ± 0.11	0.31 ± 0.05

Data are presented as mean ± standard deviation for all nerves. D_x – eigenvalues [$\times 10^{-9}$ m^2/s]; *FA* – fractional anisotropy; IE – interfascicular epineurium; *MD* – mean diffusivity [$\times 10^{-9}$ m^2/s].

Table 4. *Prolonged scanning time effect on diffusion properties.*

	D_1	D_2	D_3	*MD*	*FA*
First acquisition	0.267	0.200	0.189	0.218	0.200
Second acquisition	0.285	0.222	0.211	0.239	0.172
Δ	0.018	0.022	0.022	0.021	-0.028
(%)	(6.8)	(11.3)	(11.8)	(9.6)	(-14.2)
P value	0.009	0.0005	<0.0001	0.0005	0.01

Data are presented as means. D_x – eigenvalues [$\times 10^{-9}$ m^2/s]; *FA* – fractional anisotropy; IE – interfascicular epineurium; *MD* – mean diffusivity [$\times 10^{-9}$ m^2/s]; ns – non-significant; Δ (%) – difference between the acquisitions with proportions. Statistical analysis was conducted using repeated measures *t*-test.

Table 5. *Intra-class correlation coefficients*.

	Intra-rater ICC	Inter-rater ICC
FA of nerve	0.99	0.99
FA of fascicles	0.95	0.91

FA – fractional anisotropy; ICC – intra-class correlation coefficient.

DISCUSSION

In this study, we evaluated analysis-associated factors influencing diffusion tensors of peripheral nerves. Factors related to ROI selection or acquisition protocol significantly impacted diffusion tensors, underscoring the importance of considering these factors when interpreting the results of similar studies.

The surrounding background of MRI-acquired images consisted of a perfluorinated liquid without hydrogen atoms and produced no detectable MR signal (Awais *et al.*, 2022); however, ROI size selection significantly influenced diffusion tensors. This was likely due to the sensitivity to background noise (Alibegović *et al.*, 2024). Increasing the ROI area by 25% of the background yielded significant differences compared to values obtained when delineating only the epineurium. However, minor delineation errors should not substantially affect the diffusion tensors. It is important to note that muscle and connective tissue in vivo contain hydrogen atoms, and each tissue type exhibits distinct diffusion properties (Bihan, 1995; Seehaus *et al.*, 2015). Therefore, the inclusion of the surrounding background into the ROI could notably reduce the *FA*. To avoid such mistakes, authors also report the highest *FA* rather the the mean value (Tanitame *et al.*, 2011).

The differences between diffusion tensors of the intermediate and initial sections might be attributed to the partial volume effect. Notably, the MRI sections were 625 μm thick, and the samples not extending through the entire section are expected to show different diffusion properties, similar to delineations with the background. Moreover, the traumatic injuries caused by sample processing may affect the structural integrity and, consequently, the diffusion tensors (Prats-Galino *et al.*, 2018). Additionally, nerve positioning and twisting of fibres could influence diffusion tensors. It is also likely that the partial overlap between the initial and ending sections could interfere with the diffusion tensors. This overlap (i.e., mirror artifact) occurred due to the specific MR settings. The lower dispersion of eigenvalues observed in the intermediate nerve portions suggests that these portions are preferable for analysis over the initial sections.

Studies have shown that interfascicular epineurium exhibits lower values of *FA* compared to fascicles or perineurium, and this significantly affects the *FA* of the nerve (Awais *et al.*, 2022; Pušnik *et al.*, 2023). However, a strong positive correlation between *FA* of the fascicles and *FA* of fascicles with interfascicular epineurium indicates that differences between individuals should be able to be detected regardless of the delineation technique; nonetheless, the samples should be analysed in the same manner.

Analysis of diffusion tensors on images acquired with consecutive scans revealed differences in diffusion tensor metrics, likely attributable to prolonged scanning times. The observed increase in eigenvalues and MD with simultaneously decreased *FA* are consistent with the autolysis of cellular components. This phenomenon was anticipated and partly attributed to the extended scanning window. Immersion of samples in carbon-fluorinated liquid presumably mitigated the autolytic process and did not interfere with the MR signal due to the absence of hydrogen atoms (Awais *et al.*, 2022). It is likely that smaller-caliber nerves, such as the sural nerve (Fisse *et al.*, 2021), would be even more affected by the desiccation process. Moreover, to minimize the effect of long acquisition times, the scanning protocol was optimized by capturing all 20 images simultaneously rather than sequentially. This strategy evenly distributed any

potential volume changes across all images, minimizing the impact on the calculation of diffusion tensor indices. A shorter scanning time could reveal more comparable data between consequent scanning and should be considered in future studies; however, such protocols come with a cost of a lower signal-to-noise ratio or/and lower image resolution (Longmore, 1989; Weber *et al.*, 2021).

The presence of the referential histological image had a significant impact on the fascicle count, particularly due to the recognition of smaller fascicles hidden in the hyperintense interfascicular epineurium on T_2-weighted images. As these fascicles were small in size, their recognition is likely not important in diffusion tensor calculations; however, the influence of evaluator being blinded or unblinded to the referential image is crucial in studies that evaluate fascicle differentiation with different radiological methods (Snoj *et al.*, 2024). The slightly lower reliability of diffusion tensor measurements between two raters, which still remained high, could less likely be attributed to an overlooked fascicles. However, a more significant factor might be the delineation technique employed and the precision of the evaluator, as the perineurium and interfascicular epineurium possess diffusion tensor properties that differ considerably from those in the nerve fascicles (Awais *et al.*, 2022; Pušnik *et al.*, 2023).

This study has some limitations. First, the influence of factors associated with the MRI protocol was not evaluated, as the focus was on elucidating the impact of ROI-associated factors on diffusion tensors. Second, the ambient temperature was not strictly regulated, so minor fluctuations in room temperature could have influenced the results, especially considering the temperature dependence of diffusion. Third, the samples were obtained from cadavers with varying post-mortem intervals, which could potentially affect diffusion tensor indices.

In conclusion, the intermediate portions of nerves are recommended for diffusion tensor analysis, with manual tracing of the nerve CSA preferred over semi-automatic methods. While minor background effects can be disregarded when using an inert liquid, special attention must be given when the background comprises tissues with varying diffusion properties. Prolonged acquisition times can potentially affect diffusion tensors, highlighting the necessity for standardized pre-scanning conditions, sample handling, and acquisition protocols. Finally, consistency in delineations is paramount, regardless of whether the tracing method includes or excludes the interfascicular epineurium.

ACKNOWLEDGMENTS

We thank Majda Črnak Maasarani for technical assistance with sample processing and Chiedozie Kenneth Ugwoke for manuscript proofreading. This research was supported by the Slovenian Research and Innovation Agency (ARIS) grants P3-0043 and N3-0256.

COMPETING INTERESTS

The authors have no conflicts of interest to declare.

REFERENCES

Alibegović A, Umek N, Pušnik L, Zubiavrre Martinez I (2024). Comparison of the Visual Scoring Method and Semi-Automatic Image Analysis for Evaluating Staining Intensity of Human Cartilage Sections. Image Anal. Stereol 43:131–37.

Awais K, Snoj Ž, Cvetko E, Serša I (2022). Diffusion Tensor Imaging of a Median Nerve by Magnetic Resonance: A Pilot Study. Life 12(5):748.

Bihan D (1995). Molecular diffusion, tissue microdynamics and microstructure. NMR in Biomedicine (7-8):375–86.

Breckwoldt MO, Stock C, Xia A, Heckel A, Bendszus M, Pham M, Heiland S, Bäumer P (2015). Diffusion Tensor Imaging Adds Diagnostic Accuracy in Magnetic Resonance Neurography. Invest Radiol 50(8):498–504.

Chen H, Xu Y, Wang W, Deng R, Li Z, Xie S, Jiao J (2023). Assessment of Lumbosacral Nerve Roots in Patients with Type 2 Diabetic Peripheral Neuropathy Using Diffusion Tensor Imaging. Brain Sciences 13(5):828.

Cosottini M, Roccatagliata L (2021). Neuroimaging at 7 T: are we ready for clinical transition? Eur Radio Exp. 5(1):37.

Fisse AL, Katsanos AH, Gold R, Krogias C, Pitarokoili K (2021). Cross-sectional area reference values for peripheral nerve ultrasound in adults: A systematic review and meta-analysis—Part II: Lower extremity nerves. Eur J Neurol 28(7):2313–2318.

Gallagher TA, Simon NG, Kliot M (2015). Diffusion tensor imaging to visualize axons in the setting of nerve injury and recovery. Neurosurgical Focus 39(3):E10.

Goyal M, Samuel AJ, Mittal A (2022). Diffusion tensor imaging in patients with diabetic peripheral neuropathy: Fractional anisotropy and apparent diffusion coefficient dataset of posterior tibial nerve. Data in Brief 43:108421.

Jeon T, Fung MM, Koch KM, Tan ET, Sneag DB (2018). Peripheral nerve diffusion tensor imaging: Overview, pitfalls, and future directions. J Magn Res Imaging 47(5):1171–1189.

Koo TK, Li MY (2016). A Guideline of Selecting and Reporting Intraclass Correlation Coefficients for Reliability Research. J Chiropr Med 15(2):155–63.

Lehmann HC, Zhang J, Mori S, Sheikh KA (2010). Diffusion tensor imaging to assess axonal regeneration in peripheral nerves. Exp Neurol 223(1):238–44.

Longmore DB (1989). The principles of magnetic resonance. Br Med Bull 45(4):848–80.

Prats-Galino A, Čapek M, Reina MA, Cvetko E, Radochova B, Tubbs, RS, Damjanovska M, Stopar Pintarič T (2018). 3D reconstruction of peripheral nerves from optical projection tomography images: A method for studying fascicular interconnections and intraneural plexuses. Clin Anat 31(3):424–31.

Pušnik L, Serša I, Umek N, Cvetko E, Snoj Ž (2023). Correlation between diffusion tensor indices and fascicular morphometric parameters of peripheral nerve. Front Physiol 14:1070227.

Seehaus A, Roebroeck A, Bastiani M, Fonseca L, Bratzke H, Lori N, Vilanova A, Goebel R, Galuske R (2015). Histological validation of high-resolution DTI in human post mortem tissue. Front Neuroanat 9:98.

Snoj Ž, Pušnik L, Cvetko E, Burica Matičič U, Jengojan SA, Omejec G (2024). Sciatic nerve fascicle differentiation on high-resolution ultrasound with histological verification: An ex vivo study. Muscle Nerve 70(2):265–272.

Snoj Ž, Serša I, Maticic U, Cvetko E, Omejec G (2020). Nerve fascicle depiction at MR microscopy and high-frequency us with anatomic verification. Radiology 297:672–674.

Sveinsson B, Rowe OE, Stockmann JP, Park DJ, Lally PJ. Rosen MS, Barry RL, Eichler F, Rosen BR, Sadjadi R (2022). Feasibility of simultaneous high-resolution anatomical and quantitative magnetic resonance imaging of sciatic nerves in patients with Charcot–Marie–Tooth type 1A (CMT1A) at 7T. Muscle Nerve 66(2):206–211.

Tanitame K, Iwakado Y, Akiyama Y, Ueno H, Ochi K, Otani K, Takasu M, Date S, Awai K (2011). Effect of age on the fractional anisotropy (FA) value of peripheral nerves and clinical significance of the age-corrected FA value for evaluating polyneuropathies. Neuroradiology 54(8):815–21.

Wang X, Luo L, Xing J, Wang J, Shi B, Li YM, Li YG (2022). Assessment of peripheral neuropathy in type 2 diabetes by diffusion tensor imaging. Quant Imaging Med Surg 12(1):395–405.

Weber M, Wilhelm T, Schmidt V (2021). Multidimensional Characterisation of Time-dependent Image Data: A Case Study for the Peripheral Nervous System in Ageing Mice. Image Anal Stereol 40(2):85–94.